PROTEINS: Structure, Function, and Bioinformatics 64:749–757 (2006)

Phosphorylation-Induced Transient Intrinsic Structure in the Kinase-Inducible Domain of CREB Facilitates Its Recognition by the KIX Domain of CBP

Iván Solt, Csaba Magyar, István Simon, Peter Tompa, and Monika Fuxreiter*
Institute of Enzymology, Biological Research Center, Hungarian Academy of Sciences, Budapest, Hungary

ABSTRACT **Phosphorylation at Ser-133 of the kinase inducible domain of CREB (KID) triggers its binding to the KIX domain of CBP via a concomitant coil-to-helix transition. The exact role of this key event is still puzzling: it does not switch between disordered and ordered states, nor its direct interactions fully account for selectivity. Hence, we reasoned that phosphorylation may shift the conformational preferences of KID towards a binding-competent state. To this end we investigated the intrinsic structural properties of the unbound KID in phosphorylated and unphosphorylated forms by simulated annealing and molecular dynamics simulations. Although helical populations show subtle differences, phosphorylation reduces the flexibility of the turn segment connecting the two helices in the complexed structure and induces a transient structural element that corresponds to its bound conformation. It is stabilized by the pSer-133–Arg-131 interaction, which is absent from the unphosphorylated KID. Diminishing this coupling decreases the 3.1 kcal/mol contribution of pSer-133 to the binding free energy (ΔG_{bind}) of the phosphorylated KID to KIX by 1.1 kcal/mol, as computed in reference to Ser-133. In a binding competent form of the S133E KID mutant, the contribution of Glu-133 to ΔG_{bind} is by 1.5 kcal/mol smaller than that of pSer, suggesting that altered structural properties due to pSer → Glu replacement impair the binding affinity. Thus, we propose that phoshorylation contributes to selectivity not merely by the direct interactions of the phosphate group with KIX, but also by promoting the formation of a transient structural element in the highly conserved turn segment. Proteins 2006;64:749–757.** © 2006 Wiley-Liss, Inc.

Key words: natively unfolded protein; induced folding; molecular recognition; disorder-to-order transition; structural stability; preformed structural element

INTRODUCTION

Intrinsically unstructured/natively unfolded proteins (IUPs) lack a well-defined tertiary fold and extensive regular secondary structure, but exist as a rapidly interconverting ensemble of extended conformational states.[1–4] These extremely flexible and adaptable proteins prevail in eukaryotic proteomes,[5] and are implicated in essential biological functions. Often, they fulfil their function by interacting with a partner molecule in a process of induced folding or disorder-to-order transition, usually characterized by high specificity, fast rate, yet great reversibility.[6] This mode of recognition is primarily encountered in signaling/regulatory proteins[5,7] and chaperones.[8]

The cAMP response element binding protein (CREB) is a transcription factor that stimulates gene expression in response to cAMP signaling by associating with the KIX domain of the coactivator CBP/p300.[9] KIX recognition, localized to a short segment, the kinase-inducible domain (KID), within the largely disordered transactivator domain of CREB,[10] is evoked by the phosphorylation of Ser-133 of KID. In solution, KID itself is highly unstructured,[11] while upon complexation it folds into two short α-helices (α_A and α_B) connected by a four-residue-long turn including the critical Ser-133 residue.[12] Although phosphorylation of Ser-133 has a pivotal role in binding and folding,[10,12] its exact mechanistic role remains to be uncovered.

In vitro the affinity of the unphosphorylated KID for KIX is 0.006–0.03 times that of the phosphorylated peptide, pKID.[13] Contacts of the phosphate group with Tyr-658 and Lys-662 of KIX contribute to the binding free energy (ΔG_{bind}) by −2.8 and −1.4 kcal/mol, respectively, based on the affinity changes upon Y658F and K662A mutations.[13–15] The double mutation Y658F, K662A decreases binding affinity by almost four orders of magnitude.[14] These experiments assign a critical role to the hydrogen bond between pSer-133 and Tyr-658 in stabilizing the pKID:KIX complex. Although these interactions seem to be specific to pSer, the interpretation of these data in terms of pKID/KID selectivity is problematic due to the unknown effect of these mutations on the binding affinity of the unphosphorylated KID. For example, removing the

The Supplementary Material referred to in this article can be found at http://www.interscience.wiley.com/jpages/0887-3585/suppmat/

Grant sponsor: Wellcome Trust; Grant number: GR067595; Grant sponsor: OTKA; Grant numbers: T049073, F046164; Grant sponsor: GVOP-3.2.1.-2004-04-0195/3.0.

*Correspondence to: Monika Fuxreiter, Institute of Enzymology, Biological Research Center, Hungarian Academy of Sciences, Budapest, Hungary. E-mail: monika@enzim.hu

Received 22 December 2005; Revised 10 March 2006; Accepted 17 March 2006

Published online 7 June 2006 in Wiley InterScience (www.interscience.wiley.com). DOI: 10.1002/prot.21032

hydroxyl group of Tyr-658 does not only break a hydrogen bond with the phosphate group, but can lead to water penetration into the less tight complex that can also affect the binding free energy of the unphosphorylated KID. Reflecting this ambiguity, in contrast to other enzymes[16–18] pSer cannot be replaced by another negatively charged side chain, such as glutamate,[14] which would also be capable to maintain the critical interactions with the Y658 and K662 residues.

The discrepancy between these data suggests that phosphorylation might affect the structure of KID in such a way that its conformation is shifted towards a binding competent state. To probe this tenet, solution structures of pKID and KID were investigated by NMR measurements. The presence of the phosphate moiety however, was found to increase helicity of α_B to only a minor extent (5%).[11] It points to the importance of the structural changes detected in the vicinity of the phosphorylation site in facilitating the recognition process.

Recent studies have unveiled that many IUPs possess intrinsic residual structure,[2,19] some of which serve as preformed structural elements that correspond to the structure adopted in the bound state.[20] Although these elements are typically transient, that is, exist only a fraction of the time, such limited structural preorganization can reduce the conformational space of IUPs, and thus largely reduce the entropy penalty of their binding-induced folding.[21] Recently, the helically biased Leu-rich regions have been demonstrated to largely facilitate the binding of paxillin to the FAT domain of FAK.[22] The overstabilization of these secondary structure elements can be detrimental for binding as in $p27^{Kip1}$.[23,24] These transiently structured segments can also serve as primary contact sites (PCSs), as inferred from low-resolution structural studies.[25] These motifs, also termed as molecular recognition elements (MoREs) can be identified from irregularities in computed disorder patterns.[26,27] Twenty percent of all eukaryotic proteins and nearly 50% signaling and regulatory proteins were predicted to have α-helix-forming MoREs and bind via a mechanism similarly to p53 and Mdm2.[27]

Motivated by these considerations, we investigated the role of Ser-133 phosphorylation in partner recognition by KIX. We hypothesized that phosphorylation promotes the turn conformation towards a binding-competent form. To address this point, we have investigated the intrinsic conformational properties of the unphosphorylated and phosphorylated KID, and also compared to those of the S133E mutant by simulated annealing and constant temperature molecular dynamics simulations (MD) initiated from the bound form of pKID. In contrast to the similar values of the helical populations in the three models, the connecting turn segment exhibited significant conformational differences. The turn in pKID was less flexible than in KID and S133E KID, due to the coupling between Arg-131 and pSer-133 residues, which is absent in pKID and much less frequently occurs in S133E KID. As a consequence of the turn stabilization, formation of a transient structure in pKID is observed that resembles its bound conformation, while the turn in KID and S133E KID deviates considerably from this state. Computing the contribution of the turn residues to the binding free energy assessed the significance of the pSer-133–Arg-131 coupling in binding selectivity for pKID. Diminishing the charge–charge interaction with Arg-131 considerably reduces the contribution of pSer to ΔG_{bind}, indicating the importance of this contact in the initial encounter complex. The Glu-133 residue in a hypothetical binding-competent form of S133E KID provides only by 1.5 kcal/mol smaller contribution to ΔG_{bind} than pSer, suggesting that structural differences should also be taken into account when explaining the inactivity of this mutant.

We propose that besides promoting direct interactions, phosphorylation governs the recognition of pKID by KIX also by inducing the turn to adopt a transient structure that facilitates the binding-coupled folding process.

METHODS

Models

The NMR structure of the KID:KIX complex[12] (PDB code: 1kdx) contains a 28-residue segment (residues 119–146 of CREB) of the 60 residue-long pKID, the rest is highly flexible and not resolved. Out of the 16 models, with varying numbers of hydrogen bonds between the partners we selected the tightest complex (model 10 in PDB), where pKID establishes seven hydrogen bonds with KIX and the phosphate group at Ser-133 interacts with both Tyr-658 and Lys-662 with the shortest hydrogen bonding distances of 2.70 and 2.86 Å, respectively. Because the terminal residues in the model do not correspond to the actual termini of the chain, we placed neutral caps on the molecule, an acetyl group on the N-terminus and an N-methyl group on the C-terminus. The hydrogens were not rebuilt in the starting structure. The KID model was constructed by replacing the phosphoserine by serine. For the complex of S133E KID mutant with KIX, the corresponding pKID:KIX structure was used with glutamate substituting the phosphoserine residue while maintaining the interactions with both Tyr-658 and Lys-662. For the solution structure of the free S133E KID mutant the structure of KID resulting from the simulated annealing run (see below) was used as a starting model to avoid biasing by a preexisting turn conformation. Charges for phosphoserine were derived using the regular RESP procedure[28] averaging over the 16 side-chain conformations present in the complex structures.

Simulated Annealing and Molecular Dynamics Simulations

Charges of KID, pKID, and S133E KID models were neutralized by placing counterions (chloride and sodium) around them and then have been immersed into a rectangular cell of TIP3P waters.[29]

The systems were relaxed gradually: the waters and counterions were minimized for 7000 steepest descent steps followed by optimizing the protein for 5000 steps while decreasing the initial constraints to the original positions from 25 kcal/mol $Å^2$ to 5 kcal/mol $Å^2$ and finally

15,000 steps of unconstrained minimization was performed until the maximum gradient dropped below 1 kcal/mol Å. The temperature that is sufficient to overcome the folding barrier has been determined by some preliminary test runs. Accordingly, all relaxed models were heated from 0 to 1000 K within 50 ps, then a 350-ps molecular dynamics (MD) simulation was carried out at 1000 K then the system was cooled to 300 K within 490 ps followed by a 110-ps short MD run at 300 K. Then a 1-ns MD simulation at 300 K was performed and configurations were collected at every 0.5 ps. The structure of the unphosphorylated KID resulting from the 1-ns simulated annealing run was used as a starting model for the S133E KID mutant. After introducing the Ser-to-Glu mutation the molecule was resolvated and counterions were added. The system was relaxed by a similar protocol as KID and pKID and then was equilibrated by a 1-ns MD simulation at 300 K followed by a 1-ns production run and configurations were collected at every 0.5 ps. All simulations were carried out using NVT ensemble with AMBER 8[30] using ff94 force field,[31] because it resulted in the best agreement with the experimentally measured helical populations. Performance of other forcefields[32–35] are discussed in the Supplementary material. A step-size of 0.001 ps was used and SHAKE constraints[36] were applied on the hydrogen atoms. The electrostatic forces were calculated by the PME method[37] with a 10-Å cutoff for nonbonded interactions.

Calculation of the Binding Free Energy

To quantify the relative importance of the groups in binding of KID to KIX, the binding free energy contributions were determined for the phosphorylated and unphosphorylated Ser-133 and also for Arg-131 using the semimicroscopic version of the Protein Dipoles Langevin Dipoles (PDLD/S) method.[38,39] The difference in free energy of the respective groups in water and protein was computed as:

$$\Delta\Delta G^{w\to p} = \left[\sum_i - \Delta G^{i,\infty}_{\mathrm{sol},w} + (\Delta G^{p}_{\mathrm{sol}}(q = q_0) - \Delta G^{p}_{\mathrm{sol}}(q = 0)) \right] \cdot \left(\frac{1}{\varepsilon_{in}} - \frac{1}{\varepsilon_{w}} \right) + V_{\mu q} \frac{1}{\varepsilon_{in}}$$

where $\sum_i - \Delta G^{i,\infty}_{sol,w}$ is the solvation energy of the specific residue in water, when the charged groups are infinitely separated from each other. $\Delta G^{p}_{\mathrm{sol}}$ is the solvation energy of the studied group in protein in charged ($q = q_0$) and uncharged ($q = 0$) form (with zero residual charges). $V_{\mu q}$ is the interaction between the specific group and the protein charges and polar groups in vacuum. ϵ_w is the dielectric constant of water, and ϵ_{in} is a scale factor that represents the contributions, not considered explicitly in the model.[38,40,41] The value of ϵ_{in} was calibrated to reproduce the experimentally measured difference between $(\Delta\Delta G)^{w\to p}$ values of doubly and singly charged phosphate group in the complex:[42] $\epsilon_{\mathrm{in}} = 6$ was used throughout this study.

To account for the protein reorganization upon transferring a charged group from water to the protein site the Linear Response Approximation (LRA)[38,43] has been applied by averaging the electrostatic free energies over protein configurations generated by MD simulations:

$$\Delta\Delta G^{w\to p} = \frac{1}{2}\left(\langle \Delta\Delta G^{w\to p} \rangle_{q=q_0} + \langle \Delta\Delta G^{w\to p} \rangle_{q=0} \right)$$

where the $\langle \Delta\Delta G^{w\to p} \rangle_{q=q_0}$ and $\langle \Delta\Delta G^{w\to p} \rangle_{q=0}$ term is the average solvation energy of configurations generated when the relevant groups were charged and uncharged, respectively.

PDLD/S Simulations

Binding free energy calculations were performed within the framework of spherical boundary (SCAAS) conditions.[38,44] The relevant group, binding free energy, of which was computed was considered as Region I, whereas the rest of the complex as Region II. Region I included the side chain of Ser-133 in its phosphorylated and unphosphorylated forms, the guadinino group of Arg-131 and the side chain of Glu-133 in the S133E KID mutant. All ionizable residues were considered in their charged form. The complex was immersed into a grid of Langevin dipoles of 18.5 Å radius (Region III) with 1 and 3 Å size for the inner and outer grid, respectively, which was surrounded by continuum solvent (Region IV). The long-range interactions were treated by local reaction field (LRF) approximation.[43] The PDLD/S-LRA calculations were performed by the program MOLARIS version 9.05[39] using ENZYMIX force field[38] for the MD simulations. The $(\Delta\Delta G)^{w\to p}$ values of Region I atoms were averaged over 10 configurations, generated by 10 ps as well as 50 ps MD simulations in water and protein, respectively. An internal protein constraint of 0.3 kcal/mol Å^2 was applied on the Region II atoms to keep the system close to its original conformation. Results of the configurations generated by the first 2 ps were disregarded for averaging. The $(\Delta\Delta G)^{w\to p}$ values were converged after five to six configurations.

RESULTS

Conformational Analysis of KID, pKID, and S133E KID

In solution, both KID and pKID structures are highly disordered, with helical propensities of ~50% for α_A (residues 120–129), and only ~10% for α_B (residues 134–144) for KID and pKID, respectively.[11] Phosphorylation induces only minor changes in KID conformation, mostly at the N-terminal part of the of α_B helix, where helicity is increased by 5%. As it was demonstrated by simulation studies on model peptides such increase in helical propensity is primarily due to the electrostatic interactions between the charged group and the nearby residues.[45]

Upon eliminating the interactions with KIX, the corresponding folded pKID structure is expected to shift towards the disordered state. Helical propensities for both α_A and α_B in KID and pKID, calculated as the number of helical residues according to DSSP assignments[46]/total number of residues averaged over the configurations collected during the MD simulations are in reasonable agreement with the values that were determined based on C_α chemical shifts, although they underestimate the experi-

TABLE I. Average Helical Populations of α_A (Residues 120–129) and α_B (Residues 134–144) Segments of KID in Phosphorylated and Unphosphorylated Forms as Well as the S133E Mutant

	α_A	α_B
pKID	36.4 ± 16.8	0.80 ± 5.4
KID	29.5 ± 17.1	0.04 ± 1.1
S133E	37.3 ± 24.2	0.00 ± 0.0

mentally observed populations (Table I). Variations of the helical populations are larger than the differences between the mean values of helicity, which shields the relative preferences of pKID, KID, and S133E KID for the helical structure. Main-chain torsion angles of only Lys-136, Ile-137, and Arg-140 in pKID are shifted towards the helical state as compared to their values in KID (not shown).

Because NMR measurements indicated that structural perturbations are mostly localized to the segment linking the two helices, we investigated the conformational properties of the turn in detail. The Ramachandran maps of the main-chain torsion angles of Arg-131, Pro-132, and Ser-133 are presented in Figure 1. The distributions of the ϕ, ψ angles for Arg-130 are not presented, because these had equivalent maxima in pKID, KID, and S133E KID similar to the values ($-67°$, $-7°$) observed in the complex. Interestingly, the presence of the phosphate group had minor impact on the backbone conformations of Ser-133 and Arg-131. The ϕ, ψ distribution of Ser-133 exhibits one population in KID, while in pKID two populations can be observed for pSer-133 with ψ angles shifted by 40° apart from each other. The second population of pSer-133 is centered around $\phi = -75°$ and $\psi = 35°$, that agrees well with the experimentally observed value in the complex. Centers of the distributions for ϕ, ψ angles of Arg-131 are shifted by 10° and $-20°$ in pKID relative to KID, respectively, both a bit off their values in the complex ($-117°$, 74°). The most pronounced effect of phosphorylation can be observed in the main-chain torsion angles of Pro-132, where the ψ angle is inverted from 165° in KID to $-15°$ in pKID, which is in excellent agreement with the values in the complex. The ϕ, ψ distributions for the turn residues of S133E KID are fairly similar to those of the unphosphorylated KID. The backbone of Glu-133 is more flexible than that of Ser-133 in KID or pSer-133 in pKID, but its center of distribution deviates from the complexed structure as much as in KID. For Arg-131 in S133E KID, two conformations were observed, out of which the less populated exhibits the same conformation as Arg-131 in the pKID:KIX complex. The ϕ, ψ distribution of Pro-132 remains unaffected by the Ser → Glu substitution. The overall turn conformation was characterized by the turn width measured between the Cα atoms of residues 130 and 133 and the torsion angle computed between the Cα atoms of the consecutive residues (Θ) (Table II). The distributions of both parameters largely overlap for the unphosphorylated KID and S133E KID structures, while those of pKID are narrower and shifted towards their values in the complex. The turn width in pKID is in excellent agreement with the distance between the Cα atoms of Arg-130 and pSer-133 measured in model 10 in the pKID:KIX complex (8.83 Å).

One of the structural differences observed between the unphosphorylated and phosphorylated forms of KID in solution is a weak, but unambiguous NOE between Arg-131 and pSer-133,[11] suggesting a transient coupling between these two groups. Hence, we analyzed the separation (measured between CZ of Arg-131 and OG of pSer and Ser-133, or CG of Glu-133) and relative orientation of these two residues, respectively (Fig. 2). A stable contact between pSer-133 and Arg-131 is clearly shown in the free pKID in solution with even shorter distances than in the complex (6.5 ± 1.5 Å for all models in pKID:KIX). This interaction is obviously absent in KID, where these two residues can move freely relative to each other, indicated by their larger separation and much greater variation than in pKID (10.0 ± 1.7 Å vs. 4.8 ± 0.5 Å). The glutamate in S133E KID is a good candidate to couple with Arg-131, but due to the weaker interaction and its larger intrinsic flexibility this contact occurs with a low probability [Fig. 2(A)]. To distinguish the main-chain and side-chain effects in determining the optimal arrangement of residues 131 and 133, we have analyzed the torsion angle ϑ defined by $C_\beta(131)$–$C_\alpha(131)$–$C_\alpha(133)$–$C_\beta(133)$ in the three models [Fig. 2(B)]. The ϑ parameter indicates that Arg-131 and pSer-133 are more restricted in pKID than the corresponding residues in KID or S133E KID, reflected by the distribution widths 17° in pKID, whereas 43° and 45° in KID and S133E KID, respectively. The relative orientation of Arg-131 and pSer-133 in pKID is very close to its value $-36°$ in the pKID:KIX complex. All these parameters suggest that due to a coupling between Arg-131 and pSer-133 the turn can adopt a transient structure that presages its bound state.

Binding Free Energy Calculations

As outlined in the Introduction, the contribution of the direct interactions of the phosphate group to the selectivity of KIX for pKID cannot be deduced quantitatively from the mutagenesis experiments due to the lack of data pertaining to the unphosphorylated form. Although the phosphate group is inevitably a dominant factor in binding of pKID to KIX, it appears that additional contacts are also required for full competence. The roles of different groups in determining the affinity of pKID for KIX were elucidated by computing their contribution in pKID, KID, and S133E KID to the binding free energy to KIX using the semimicroscopic version of the Protein Dipoles Langevin Dipoles (PDLD/S) method.[38] The results are summarized in Table III.

The stability of the calculations was tested by averaging the solvation free energy differences upon moving the respective groups from water to their protein site ($\Delta\Delta G^{w\to p}$) over MD simulations of different lengths. The averages obtained over configurations derived from 10 and 50 ps simulations (10 each) agree within 0.3 kcal/mol (see the corresponding lines in Table III with *a* and *b* superscripts), indicating that the calculations are converged. The error

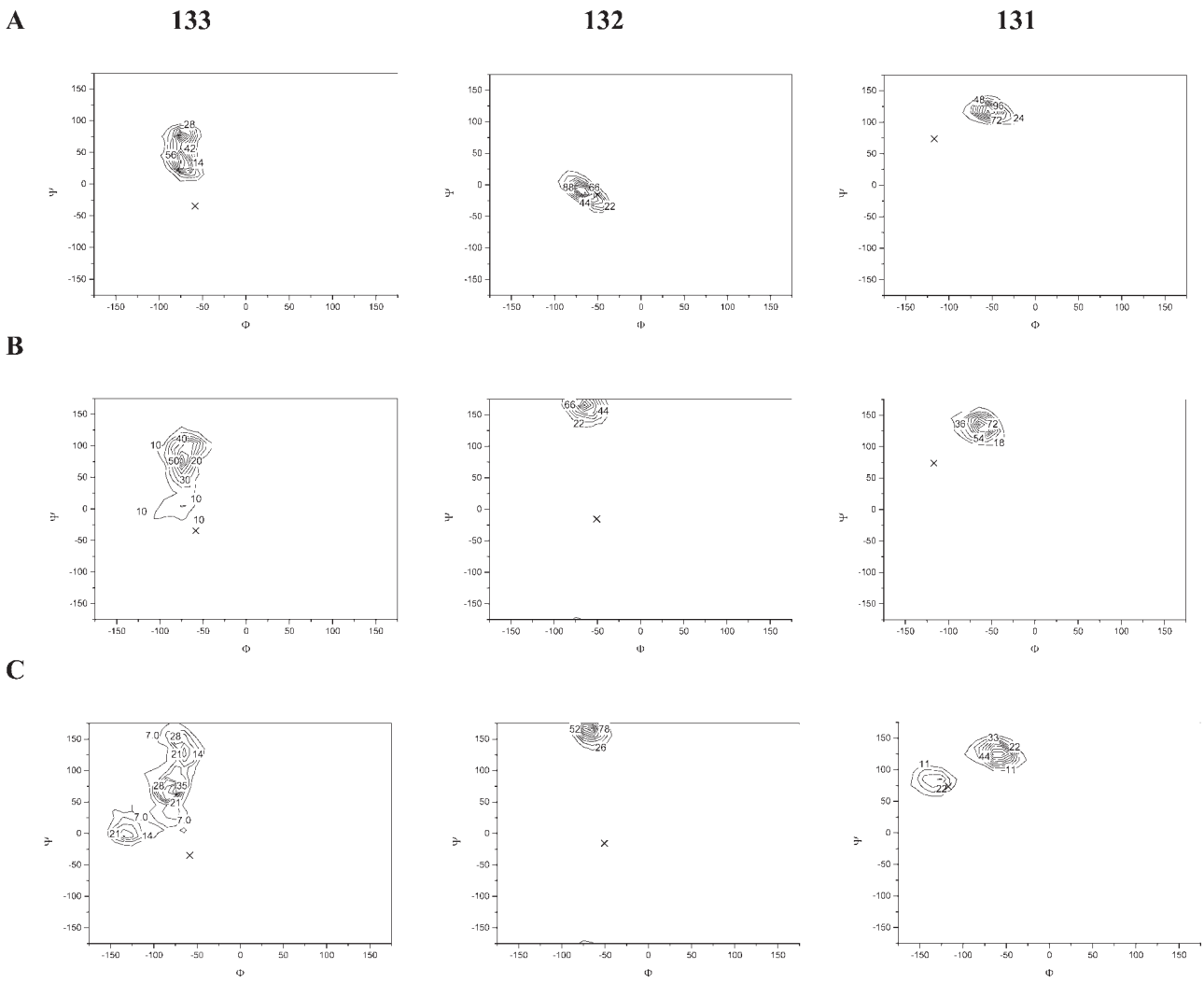

Fig. 1. ϕ,ψ distribution of main-chain torsion angles of the 131–133 turn residues in (**A**) pKID, (**B**) KID, and (**C**) S133E KID. Residue 133 is pSer in pKID, Ser in KID, and Glu in S133E KID. The corresponding torsion angles in the pKID:KIX complex are marked by crosses (for Pro-132 in pKID they overlap).

TABLE II. Turn Conformation Characterized by the Turn Width (W) Defined as the Distance between the C_α(130) and C_α(133) and the Torsion Angle (Θ) Defined by the Consecutive C_α Atoms of Residues 130–133

	W (Å)	Θ (°)
pKID	8.83 ± 0.26	−142.9 ± 10.4
KID	9.45 ± 0.43	−115.8 ± 16.2
S133E	9.63 ± 0.39	−121.5 ± 57.5
pKID:KIX	9.06 ± 0.32	−143.5 ± 77.0

The pKID:KIX refers to the average of the 16 models in 1kdx.pdb.[16]

range of the calculations can be estimated as 0.2 kcal/mol from the difference between the $\Delta\Delta G^{w\to p}$ values upon moving a doubly charged and a singly protonated phosphoserine group to their site in the pKID:KIX complex compared to the experimental data of 1.5 kcal/mol.[42]

The contributions of different functional groups to the binding free energy ($\Delta\Delta G_{\text{bind}}$) were derived as the difference between the $\Delta\Delta G^{w\to p}$ values obtained upon moving the relevant groups from water to KID and to the KID:KIX complex, respectively. The contribution of the phosphate group to ΔG_{bind} is −2.8 kcal/mol, while the interactions of the unphoshorylated Ser-133 give an almost negligible unfavorable contribution of 0.3 kcal/mol. Accordingly, the presence of the phosphate group decreases the binding free energy by 3.1 kcal/mol more than that of the OH group in the unphosphorylated KID, leading to three orders of magnitude difference in the binding affinities in good agreement with the experimental results.[13,14]

Our calculations show that the contribution of the phosphate group can provide almost half of the total −7.6 kcal/mol binding free energy,[13] by taking the effect of all the interactions of the phosphate group with all groups in KIX in reference to those of the OH group of Ser-133 of KID into account. This contribution is by 1.3 kcal/mol smaller than the value derived from the affinity change upon the double mutation Y658F, K662A of KIX.[14] The discrepancy between the computed and experimental values illustrates

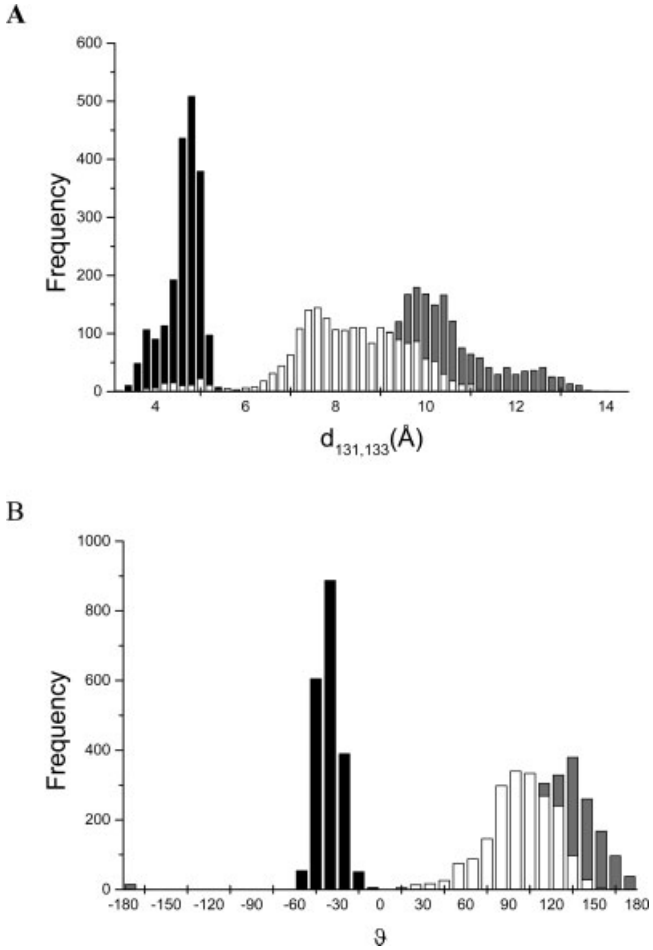

Fig. 2. Separation and relative orientation of Arg-131 and pSer-133 in pKID (black), Ser-133 in KID (gray), and Glu-133 in S133E KID (hollow) characterized by the (**A**) distance between CZ of Arg-131 and the OG in pKID and KID and CG in S133E KID, respectively, and (**B**) the torsion angle ϑ defined by $C_\beta(131)$–$C_\alpha(131)$–$C_\alpha(133)$–$C_\beta(133)$.

TABLE III. Free Energy Contributions of Functional Groups to the Binding Free Energy

Region 1	$\Delta\Delta G^{w\to p}$ (KID)	$\Delta\Delta G^{w\to p}$ (KID:KIX)	$\Delta\Delta G^{\text{bind}}$ (KID:KIX)
C_β-PO_4^{2-a}	−3.42	−6.59	−3.17
C_β-OH[a]	0.40	0.60	0.20
C_β-$PO_4^{2-a,c}$	1.35	6.13	4.78
C_β-OH[a,c]	0.42	0.70	0.28
C_β-PO_4^{2-b}	−3.46	−6.31	−2.85
C_β-$PO_3(OH)^{-b}$	−2.55	−3.74	−1.19
C_β-OH[b]	0.37	0.63	0.26
Arg-131[b,c]	0.76	0.19	−0.57
C_β-$PO_4^{2-b,d}$	−0.83	−2.60	−1.77
Glu-133^{-b}	−1.93	−3.27	−1.34

$\Delta\Delta G^{W\to P}$ are the free energies of moving the groups from water to their protein site in KID, pKID, S133E KID, and in KID:KIX complex, respectively. $\Delta\Delta G^{\text{bind}} = \Delta\Delta G^{\text{w}\to\text{p}}$ (KID:KIX) − $\Delta\Delta G^{w\to P}$ (KID).
[a]Averaging over 10 MD simulations 10 ps each.
[b]Averaging over 10 MD simulations 50 ps each.
[c]All ionizable residues in KID and KIX are neutral.
[d]Arg-131 is neutral.
[e]Guanidino group of Arg-131.

that the latter reflects two opposite, but not canceling effects: while Y658F creates an apolar evironment, in K662A more water molecules penetrate to the binding site.

Besides the phosphoserine group, Arg-131 also provides a smaller, favorable contribution of −0.6 kcal/mol to binding free energy of pKID to KIX. Neutralizing the positive charge of the guanidino group of Arg-131, however, reduces the stabilization of the phosphate group substantially, by 3.7 kcal/mol in the pKID:KIX complex, while $\Delta\Delta G^{w\to p}$ of the phosphate group in free pKID is affected to a lesser extent. Overall, removing the coupling between the phosphate group and the charged guanidino group of Arg-131 decreased the ΔG_{bind} of pKID by 1.1 kcal/mol. Thus, the pSer-133–Arg-131 interaction enhances the formation of the pKID:KIX complex.

The key importance of charge–charge interactions in binding of KID to KIX in general was demonstrated by turning off the permanent charges of the ionizable residues in KID and KIX, respectively. This change left ΔG_{bind} of Ser-133 in KID almost unaffected (0.3 kcal/mol), while it resulted in a dramatic destabilization of the phosphate group in the pKID:KIX complex by 4.8 kcal/mol unfavorable contribution to the binding free energy.

To elucidate the origin of incompatibility of the S133E mutant, the contribution of Glu-133 to the binding free energy to KIX was also determined assuming that pSer → Glu substitution does not affect the conformation of either the KID or the KIX structure. Thus, $\Delta\Delta G_{\text{bind}}$ was calculated in a hypothetical model that represents a fully binding-competent state for S133E KID reflecting only changes in the electrostatic effects. The pSer to Glu replacement decreased the binding free energy contribution of this residue by 1.5 kcal/mol in excellent agreement with free energy changes upon protonating the doubly charged phosphate group.[42] The discrepancy between the complete loss of activity of the S133E KID mutant,[14] and the only 12-fold change in affinity due to electrostatic effects suggest that the substitution of pSer by Glu is accompanied by a conformational transition that impairs complementarity at the KID:KIX interface.

DISCUSSION

Molecular recognition by IUPs is a key element of their functioning that is often coupled to a structural transition from a disordered to an ordered bound state.[1–4,6] This type of recognition can also be regarded as a special case of folding. The intrinsic flexibility of IUPs confers several advantages in the binding process, by providing excessive and malleable binding surface for the partner and by increasing the speed of interaction. Too much flexibility, however, would be detrimental to effective binding, primarily due to entropic reasons. To reconcile these seemingly contradictory notions it has been raised recently that many IUPs are not fully unstructured, but exhibit functionally relevant residual structure.[2,19] These transiently ordered segments, so-called preformed structural elements,[20] provide either thermodynamic or kinetic benefits for binding in the form of MoREs[26,27] or PCSs.[25] These elements not only decrease the entropy penalty of folding but also

can increase the probability of formation of a binding competent conformational state. These segments can ideally serve as 'first contact points' by offering complementary binding surfaces to the partner. Within the framework of the 'fly-casting' mechanism,[47] limiting the conformational freedom upon the formation of the initial encounter complex serves to eliminate the kinetic traps along the folding pathway. In other words, such association creates a new transition state for binding with decreased number of nonspecific contacts.[21]

This mode of binding may be benefited in various biological settings, such as the inducible association of KID to its partner, KIX. KID is a short segment within the longer (about 265 AAs) disordered trans-activator domain of CREB. Its binding to the KIX domain of CBP triggered by phosphorylation is accompanied by a disorder-to-order transition due to changing from a random coil to a mostly helical structure.[12] It has been demonstrated that intrinsic disorder in general enhances susceptibility for phosphorylation.[48] Phosphorylation of Ser-133 of KID has only a minor impact on the helix content of the domain in solution.[11] The critical role of phosphorylation was attributed to the favorable interaction between the phosphate moiety and Tyr-658 and Lys-662 of KIX, assumed to be sufficient to overcome the unfavorable entropic barrier of folding. As outlined in the Introduction, however, this effect has not been unambiguously elucidated; for example, it was not quantified in reference to the unphosphorylated form. Furthermore, direct interactions of the phosphate group as exquisite determinants of selectivity cannot explain the impaired affinity of S133E KID mutant, because the glutamate residue is also capable to establish simultaneous contacts with the critical KIX residues in the complex. Thus, we hypothesized that phosphorylation is distinguished in the recognition of KID by KIX not merely by its direct interactions but also by virtue of shifting the conformational preferences towards a binding-competent state. As described above, formation of a transient structural element can be beneficial for folding-coupled binding both thermodynamically and kinetically.

To explore these possibilities, we probed the intrinsic conformational properties of the pKID and KID structures in solution and compared to those of the S133E model. All structures become largely unfolded upon simulated annealing resulting in helical propensities that slightly underestimate the experimentally measured populations. Due to the large variation of the mean helicity values, the relative preference of pKID, KID, and S133E KID towards the helical state (and thus the effect of a negatively charged group with double or single charge on the helicity of the N termini of α_B) cannot be assessed. In contrast, the turn linking the two helical segments with a highly conserved sequence displayed striking dissimilarity between the three models. The turn is less flexible in pKID than in KID or S133E KID, as witnessed by the range of turn width and the torsion angle parameters. Furthermore, the mean values of these structural descriptors in pKID were in accord with those in the pKID:KIX complex and deviated considerably from those in the unphosphorylated KID and S133E KID models. Thus, phosphorylation induces formation of a transient structural element in the turn segment that corresponds to its bound state. The proposed change in the turn conformation is also consistent with the results of limited proteolysis experiments, which show the preferential accessibility of the turn in full-length CREB that slightly changes upon phosphorylation.[49] The distinguished role of the turn is also supported by protein grafting: unphosphorylated model peptides mimicking the turn conformation have only twofold lower affinity for KIX than pKID.[50] It is worthwhile to note, that all peptide variants with considerable affinity for KIX have Arg at position 131.

This transient turn conformation is stabilized by the interaction between Arg-131 and pSer-133 in agreement with the weak NOE observed between these two residues.[11] This coupling is obviously absent in the unphosphorylated KID, and is also less frequent in S133E KID, due to the larger flexibility of Glu-133 and its weaker interaction with Arg131 (Fig. 3). Thus, we propose that the low-probability occurrence of this buttressing interaction is also responsible for the loss of affinity of S133E KID for KIX.

The significance of the coupling between pSer-133 and Arg-131 in enhancing the binding affinity of KIX was appraised based on the contributions of the turn residues to the binding free energy. We found that the presence of the phosphate group in pKID is stabilized by 3.1 kcal/mol more than the OH group in KID, while Glu provides by 1.5 kcal/mol smaller contribution to ΔG_{bind} in a hypothetical binding competent form of S133E KID than pSer in pKID, accounting only for a ~10-fold reduction in binding affinity to KIX. The inactivity of S133E KID suggests that the Glu substitution is accompanied by conformational changes that are detrimental to binding. Arg-131 has been demonstrated to provide important contribution to the binding free energy of pKID: −0.6 kcal/mol via direct interactions with KIX and −1.1 kcal/mol via coupling with the phosphoserine group. Thus, formation of the transient structural element in the turn segment of pKID does not only provide complementary interface for KIX, but is also needed to fortify the interactions between the phosphate moiety and the KIX residues. These increased enthalpic contributions in the initial encounter complex translate into lower entropic penalty of folding that facilitates the complete binding process.

In summary, based on all these results we propose that the turn in KID functions as an inducible structural motif that forms upon phosphorylation. This transient conformation presages its final bound state thus presents a complementary binding surface for KIX. We propose that the turn segment acts as a primary contact site that establishes interactions with KIX first. Contacts of the phosphate group play dominant, but not exquisite role in selectivity, the buttressing interactions with Arg-131 are also required for full competence. The enthalpic gain by the interactions in the initial encounter complex lowers the entropic penalty of folding thus accelerating the formation of the helices. Furthermore, we hypothesize that the

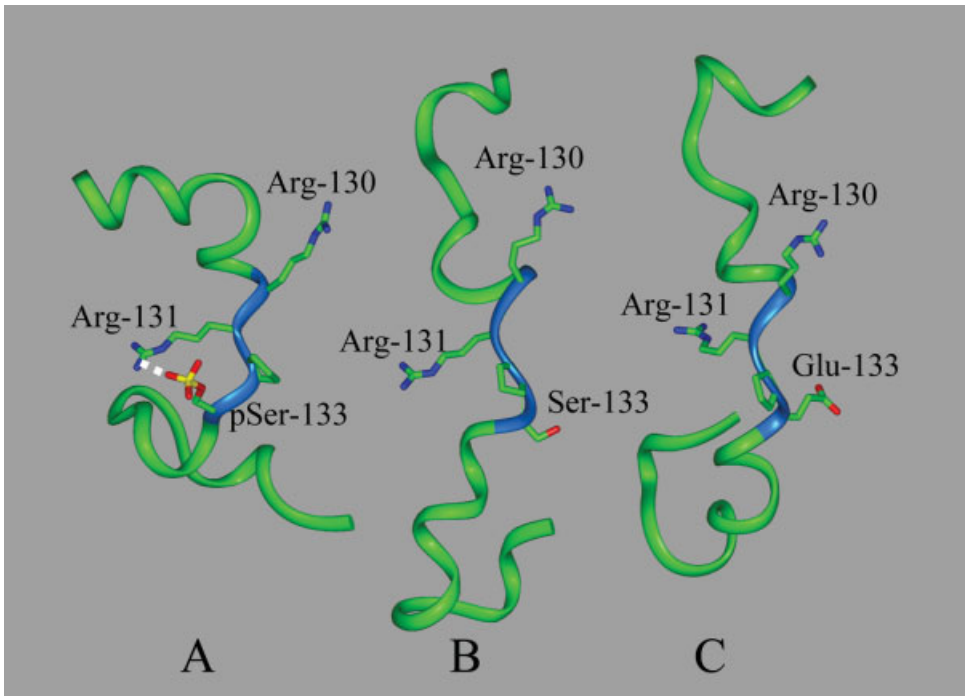

Fig. 3. Representative configurations of the (**A**) pKID (**B**) KID, and (**C**) S133E KID models. The turn is displayed by blue. In pKID, a hydrogen bond is maintained between pSer-133 and Arg-131 (marked by white dotted line).

reduced flexibility of the turn can also restrict the orientation of the connected segments that can also contribute to lowering the folding barrier upon binding. The pivotal role of the turn as a preformed structural element, rather than only the direct interactions of the phosphate group, can also rationalize why the S133E KID mutant cannot evoke a biological response. In essence, the case of KID offers an intriguing example of how IUPs exploit the presence of short but critical recognition elements for their effective binding.

ACKNOWLEDGMENTS

This work was supported by a Bolyai János fellowship (for P.T. and M.F.). The computer facility of the national supercomputer center (NIIF) is gratefully acknowledged.

REFERENCES

1. Wright PE, Dyson HJ. Intrinsically unstructured proteins: reassessing the protein structure–function paradigm. J Mol Biol 1999;293:321–331.
2. Uversky VN. Natively unfolded proteins: a point where biology waits for physics. Protein Sci 2002;11:739–756.
3. Dunker AK, Brown CJ, Lawson JD, Iakoucheva LM, Obradovic Z. Intrinsic Disorder and protein function. Biochemistry 2002;41: 6573–6582.
4. Tompa P. Intrinsically unstructured proteins. Trends Biochem Sci 2002;27:527–533.
5. Ward JJ, Sodhi JS, McGuffin LJ, Buxton BF, Jones DT. Prediction and functional analysis of native disorder in proteins from the three kingdoms of life. J Mol Biol 2004;337:635–645.
6. Dyson HJ, Wright PE. Coupling of folding and binding for unstructured proteins. Curr Opin Struct Biol 2002;12:54–60.
7. Iakoucheva L, Brown C, Lawson J, Obradovic Z, Dunker A. Intrinsic disorder in cell-signaling and cancer-associated proteins. J Mol Biol 2002;323:573–584.
8. Tompa P, Csermely P. The role of structural disorder in the function of RNA and protein chaperones. FASEB J 2004;18:1169–1175.
9. Chrivia JC, Kwok RP, Lamb N, Hagiwara M, Montminy MR, Goodman RH. Phosphorylated CREB binds specifically to the nuclear protein CBP. Nature 1993;365:855–859.
10. Parker D, Ferreri K, Nakajima T, LaMorte VJ, Evans R, Koerber SC, Hoeger C, Montminy MR. Phosphorylation of CREB at Ser-133 induces complex formation with CREB-binding protein via a direct mechanism. Mol Cell Biol 1996;16:694–703.
11. Radhakrishnan I, Perez-Alvarado GC, Dyson HJ, Wright PE. Conformational preferences in the Ser133-phosphorylated and non-phosphorylated forms of the kinase inducible transactivation domain of CREB. FEBS Lett 1998;430:317–322.
12. Radhakrishnan I, Perez-Alvarado GC, Parker D, Dyson HJ, Montminy MR, Wright PE. Solution structure of the KIX domain of CBP bound to the transactivation domain of CREB: a model for activator:coactivator interactions. Cell 1997;91:741–752.
13. Zor T, Mayr BM, Dyson HJ, Montminy MR, Wright PE. Roles of phosphorylation and helix propensity in the binding of the KIX domain of CREB-binding protein by constitutive (c-Myb) and inducible (CREB) activators. J Biol Chem 2002;277:42241–42248.
14. Parker D, Jhala US, Radhakrishnan I, Yaffe MB, Reyes C, Shulman AI, Cantley LC, Wright PE, Montminy M. Analysis of an activator:coactivator complex reveals an essential role for secondary structure in transcriptional activation. Mol Cell 1998;2:353–359.
15. Parker D, Rivera M, Zor T, Henrion-Caude A, Radhakrishnan I, Kumar A, Shapiro LH, Wright PE, Montminy M, Brindle PK. Role of secondary structure in discrimination between constitutive and inducible activators. Mol Cell Biol 1999;19:5601–5607.
16. Wei J, Davis KM, Wu H, Wu JY. Protein phosphorylation of human brain glutamic acid decarboxylase (GAD)65 and GAD67 and its physiological implications. Biochemistry 2004;43:6182–6189.
17. Hao M, Lowy AM, Kapoor M, Deffie A, Liu G, Lozano G. Mutation of phosphoserine 389 affects p53 function in vivo. J Biol Chem 1996;271:29380–29385.
18. Maciejewski PM, Peterson FC, Anderson PJ, Brooks CL. Mutation

of serine 90 to glutamic acid mimics phosphorylation of bovine prolactin. J Biol Chem 1995;270:27661–27665.
19. Tompa P. The functional benefits of protein disorder. J Mol Struct (Theochem) 2003;666–667:361–371.
20. Fuxreiter M, Simon I, Friedrich P, Tompa P. Preformed structural elements feature in partner recognition by intrinsically unstructured proteins. J Mol Biol 2004;338:1015–1026.
21. Pontius BW. Close encounters: why unstructured, polymeric domains can increase rates of specific macromolecular association. Trends Biochem Sci 1993;18:181–186.
22. Bertolucci CM, Guibao CD, Zheng J. Structural features of the focal adhesion kinase–paxillin complex give insight into the dynamics of focal adhesion assembly. Protein Sci 2005;14:644–652.
23. Verkhivker GM, Bouzida D, Gehlhaar DK, Rejto PA, Freer ST, Rose PW. Simulating disorder–order transitions in molecular recognition of unstructured proteins: where folding meets binding. Proc Natl Acad Sci USA 2003;100:5148–5153.
24. Verkhivker GM. Protein conformational transitions coupled to binding in molecular recognition of unstructured proteins: deciphering the effect of intermolecular interactions on computational structure prediction of the p27Kip1 protein bound to the cyclin A-cyclin-dependent kinase 2 complex. Proteins 2005;58:706–716.
25. Csizmok V, Bokor M, Banki P, Klement É, Medzihradszky KF, Friedrich P, Tompa K, Tompa P. Primary contact sites in intrinsically unstructured proteins: the case of calpastatin and microtubule-associated protein 2. Biochemistry 2005;44:3955–3964.
26. Bracken C, Iakoucheva LM, Romero PR, Dunker AK. Combining prediction, computation and experiment for the characterization of protein disorder. Curr Opin Struct Biol 2004;14:570–576.
27. Oldfield CJ, Cheng Y, Cortese MS, Romero P, Uversky VN, Dunker AK. Coupled folding and binding with alpha-helix-forming molecular recognition elements. Biochemistry 2005;44:12454–12470.
28. Cieplak P, Cornell WD, Bayly CI, Kollman PA. Application to the multimolecule and multiconformational RESP methodology to biopolymers: charge derivation for DNA, RNA and proteins. J Comp Chem 1995;16:1357–1377.
29. Jorgensen WL, Chandrasekhar J, Madura J, Klein ML. Comparison of simple potential functions for simulating liquid water. J Chem Phys 1983;79:926–935.
30. Case DA, Darden TA, Cheatham TE III, Simmerling CL, Wang J, Duke RE, Luo R, Merz KM, Wang B, Pearlman DA, Crowley M, Brozell S, Tsui V, Gohlke H, Mongan J, Hornak V, Cui G, Beroza P, Schafmeister C, Caldwell JW, Ross WS, Kollman PA. AMBER 8. 8. San Francisco: University of California; 2004.
31. Cornell WD, Cieplak P, Bayly CI, Kollman PA. Application of RESP charges to calculate conformational energies, hydrogen bond energies and free energies of solvation. J Am Chem Soc 1993;115:9620–9631.
32. Wang J, Cieplak P, Kollman PA. How well does a restrained electrostatic potential (RESP) model perform in calculating conformational energies of organic and bioorganic molecules? J Comp Chem 2000;21:1049–1074.
33. Garcia AE, Sanbonmatsu KY. α-Helical stabilization by side chain shielding of backbone hydrogen bonds. Proc Natl Acad Sci USA 2002;99:2782–2787.
34. Simmerling C, Strockbine B, Roitberg AE. All-atom structure prediction and folding simulations of a stable protein. J Am Chem Soc 2002;124:11258–11259.
35. Duan Y, Wu C, Chowdhury S, Lee MC, Xiong G, Zhang W, Yang R, Cieplak P, Luo R, Lee T, Caldwell J, Wang J, Kollman P. A point-charge force field for molecular mechanics simulations of proteins based on condensed-phase quantum mechanical calculations. J Comput Chem 2003;24:1999–2012.
36. Ryckaert J-P, Ciccotti G, Berendsen HJC. Numerical integration of the cartesian equations of motion of a system with constraints: Molecular dynamics of n-alkenes. J Comp Phys 1977;23:327–341.
37. Darden TA, York D. Particle mesh Ewald—an Nlog(N) method for Ewald sums in large systems. J Chem Phys 1993;103:8577–8593.
38. Lee FS, Chu ZT, Warshel A. Microscopic and semimicroscopic calculations of electrostatic energies in proteins by polaris and enzymix programs. J Comp Chem 1993;14:161–185.
39. Sham YY, Chu ZT, Tao H, Warshel A. Examining methods for calculations of binding free energies: LRA, LIE, PDLD-LRA, and PDLD/S-LRA calculations of ligands binding to an HIV protease. Proteins 2000;39:393–407.
40. King G, Lee FS, Warshel A. Microscopic simulations of macroscopic dielectric constants of solvated proteins. J Chem Phys 1991;95:4366–4377.
41. Muegge I, Schweins T, Langen R, Warshel A. Electrostatic control of GTP and GDP binding in the oncoprotein p21ras. Structure 1996;4:475–489.
42. Mestas SP, Lumb KJ. Electrostatic contribution of phosphorylation to the stability of the CREB–CBP activator–coactivator complex. Nat Struct Biol 1999;6:613–614.
43. Lee FS, Warshel A. A local reaction field method for fast evaluation of long-range electrostatic interactions in molecular simulations. J Chem Phys 1992;97:3100–3107.
44. King G, Warshel A. A surface constrained all-atom solvent model for effective simulations of polar solutions. J Chem Phys 1989;91:3647–3661.
45. Smart JL, McCammon JA. Phosphorylation stabilizes the N-termini of α-helices. Biopolymers 1999;49:225–233.
46. Kabsch W, Sander C. Dictionary of protein secondary structure: pattern recognition of hydrogen-bonded and geometrical features. Biopolymers 1983;22:2577–2637.
47. Shoemaker BA, Portman JJ, Wolynes PG. Speeding molecular recognition by using the folding funnel: the fly-casting mechanism. Proc Natl Acad Sci USA 2000;97:8868–8873.
48. Iakoucheva LM, Radivojac P, Brown CJ, O'Connor TR, Sikes JG, Obradovic Z, Dunker AK. The importance of intrinsic disorder for protein phosphorylation. Nucleic Acids Res 2004;32:1037–1049.
49. Richards JP, Bachinger HP, Goodman RH, Brennan RG. Analysis of the structural properties of cAMP-responsive element-binding protein (CREB) and phosphorylated CREB. J Biol Chem 1996;271:13716–13723.
50. Rutledge SE, Volkman HM, Schepartz A. Molecular recognition of protein surfaces: high affinity ligands for the CBP KIX domain. J Am Chem Soc 2003;125:14336–14347.